Slit2 Promotes Angiogenic Activity Via the Robo1-VEGFR2-ERK1/2 Pathway in Both In Vivo and In Vitro Studies

Shanshan Li,[1] Lvzhen Huang,[1] Yaoyao Sun,[1] Yujing Bai,[1] Fei Yang,[1] Wenzhen Yu,[1] Fangting Li,[1] Qi Zhang,[1] Bin Wang,[1] Jian-Guo Geng,[2] and Xiaoxin Li[1]

[1]Department of Ophthalmology, Peking University People's Hospital; Key Laboratory of Vision Loss and Restoration, Ministry of Education; Beijing Key Laboratory of Diagnosis and Therapy of Retinal and Choroid Diseases, Beijing, China
[2]Department of Biologic and Materials Sciences, University of Michigan School of Dentistry, Ann Arbor, Michigan, United States

Correspondence: Xiaoxin Li, Department of Ophthalmology, Peking University People's Hospital, Xizhimen South Street 11, Xi Cheng District, 100044 Beijing, China; drlixiaoxin@163.com.

SL, LH, YS, and YB contributed equally to the work presented here and therefore should be regarded as equivalent first authors.

Submitted: December 2, 2014
Accepted: June 28, 2015

Citation: Li S, Huang L, Sun Y, et al. Slit2 promotes angiogenic activity via the Robo1-VEGFR2-ERK1/2 pathway in both in vivo and in vitro studies. *Invest Ophthalmol Vis Sci*. 2015;56:5210–5217. DOI:10.1167/iovs-14-16184

Purpose. Recent research has provided novel but contrary insight into the function of Slit2-Robo signaling in angiogenesis. Although the role of Robo in choroidal neovascularization (CNV) has been studied, the effect of its ligand, Slit2, on CNV development is unclear. This study investigated the role of endogenous Slit2 in CNV and the possible mechanisms.

Methods. Laser-induced CNV in Slit2 transgenic and wild-type mice was used to study the effects of endogenous Slit2 on angiogenesis in vivo. Fluorescein angiography was performed to evaluate the leakage area of each lesion. Plasmid-based gene transfer technology was used to increase Slit2 expression and to study its effects on human umbilical vein endothelial cells (HUVECs) in vitro. Cell proliferation, migration, and tube formation were assessed. Quantitative real-time PCR and Western blot were used to measure expression in the extracellular signal-related kinase 1/2 (ERK1/2), protein kinase B (AKT), and p38 mitogen-activated protein kinase (p38 MAPK) molecular pathways.

Results. Laser treatment led to more CNV and vascular leakage in Slit2 transgenic mice compared with wild-type mice. Upregulation of Slit2, Robo1, VEGF receptor 2 (VEGFR2), and phosphorylated ERK1/2 (p-ERK1/2) were detected in retina and choroidal tissue of laser-treated transgenic mice. After transfection of HUVECs with a Slit2 overexpression plasmid, cell proliferation, migration, and tube formation capacities were promoted. Slit2, Robo1, VEGFR2, and p-ERK1/2 were elevated in transfected HUVECs.

Conclusion. Slit2 overexpression promoted angiogenic effects in both a laser-induced CNV mouse model and HUVECs and promoted the biological activity of endothelial cells. Slit2 may promote angiogenesis by upregulating Robo1 and activating the VEGFR2-ERK1/2 pathway.

Keywords: Slit2, angiogenesis, Robo1, VEGFR2

Age-related macular degeneration (AMD) is the leading cause of visual loss in elderly people in the Western world.[1] Choroidal neovascularization (CNV) occurs in the neovascular form of macular degeneration, which comprises 10% of AMD cases but accounts for 90% of the legal blindness cases attributed to AMD.[2,3] Vascular endothelial growth factor (VEGF) is a major factor in the development of wet AMD, and its overexpression is known to regulate formation of the CNV.[4]

Secreted glycoprotein Slit2 was originally identified as an axonal repellent in central nervous system (CNS) development[5–8] and has four cognate roundabout receptors, Robo1 to Robo4.[9] The role of the Slit2-Robo signaling pathway has been documented in neuronal migration during development.[10,11] Evidence has shown that Robo1 and Robo4 are expressed on endothelial cells, and the Slit2-Robo signaling pathway has been implicated in angiogenesis.[12,13] In recent years, growing interest in the effects of this signaling pathway has focused on its role in the regulation of vascular structure and function.[14] Although multiple studies have confirmed that Slit2-Robo signaling participates in angiogenesis regulation, both pro- and antiangiogenic activities of Slit2 have been reported.[15–19] The specific effects of Slit2 on endothelial cells and the molecular mechanisms of this secreted glycoprotein in angiogenesis remain unclear. The involvement of Slit2 in CNV is also unclear.

In this study, we provide insights into the role of the Slit2-Robo signaling pathway in angiogenesis using a laser-induced CNV model and human umbilical vein endothelial cells (HUVECs). According to our results, Slit2 overexpression is critical to the angiogenesis process. We also demonstrate that the proangiogenic effects of endogenous Slit2 are generated through the upregulation of Robo1 and activation of the VEGF receptor 2 (VEGFR2)-extracellular signal-related kinase 1/2 (ERK1/2) pathway. These promising results suggest Slit2-Robo1 as a potential therapeutic target for retina/choroidal angiogenic diseases.

Methods

Ethics Statement

All animal experiments were performed in adherence with the ARVO statements for the Use of Animals in Ophthalmology and Vision Research and the Institutional Animal Care and Use Committee of Peking University. All procedures were approved by the Animal Care and Use Committee of Peking University People's Hospital (Beijing, China).

Slit2 Transgenic Mice

Slit2 knockout mice are either embryonically lethal or die within 1 or 2 weeks of birth.[20] Slit2 transgenic (Tg) mice were used in this study to investigate the role of Slit2 in angiogenesis. Slit2 Tg mice (kindly provided by J.G. Geng) were generated in a C57BL/6 wild-type (WT) background according to standard procedures and were characterized as reported previously.[21,22] Briefly, the transgene was constructed by cloning the full length of human Slit2 cDNA into the pCEP4F vector, which was injected into the pronuclei of fertilized C57×CBA F1 oocytes. Genotypes were confirmed by PCR analysis and Southern blot. We used C57BL/6 mice as WT control, and the Tg mice were physiologically comparable to WT mice. The Slit2 gene had more than 90% homology among different species, and previous studies had demonstrated the interaction between human Slit2 and mouse Robos.[13]

Laser-Induced CNV Mouse Model

Laser-induced CNV lesions were performed on adult Slit2 Tg and C57BL/6 mice (male, 8 weeks old), which were given free access to food and water. Choroidal neovascularization was induced by laser photocoagulation (532 nm, 150 mW, 50 ms, 50 μm). Five lesions were made 2 PD away from the optic disc on one eye of each mouse. The morphologic end point of the laser injury was dictated by the appearance of a cavitation bubble, which is thought to be correlated with the disruption of Bruch's membrane.

Fluorescein Angiography

Fourteen days after photocoagulation, the CNV leakage areas of laser lesions were evaluated using fluorescein angiography (FA) with a Phoenix Micron IV Retinal Imaging Microscope (Phoenix, Pleasanton, CA, USA) according to the manufacturer's illustrations. Five minutes after intraperitoneal injection of 0.03 mL of fluorescein sodium (FLUORESCITE Injection; Alcon, Fort Worth, TX, USA), FA was performed. Images were analyzed using ImageJ software (http://imagej.nih.gov/ij/; provided in the public domain by the National Institutes of Health, Bethesda, MD, USA).

Cell Culture and Plasmid Transfection

We obtained HUVECs from the American Type Culture Collection (CRL-1730; ATCC, Manassas, VA, USA) and they were cultured in RPMI 1640 medium (1640; Gibco, Invitrogen, Grand Island, NY, USA) with 10% fetal bovine serum (FBS; Gibco, Invitrogen) at 37°C in 5% CO_2 and 95% humidity, as recommended by ATCC. The HUVECs were plated in six-well culture dishes and were used for experiments at 80% to 90% confluence. The HUVECs were transfected with Slit2 plasmid DNA (TrueORF cDNA clones vector, RG220894; OriGene, Rockville, MD, USA). Transfections were performed using the TurboFectin 8.0 transfection reagent (OriGene) according to the manufacturer's protocol.

Cell Proliferation Assay

The cell proliferation assay was performed as described previously.[23] The HUVECs were incubated in 96-well plates. Cell Counting Kit-8 (CCK-8; Dojindo, Shanghai, China) assays were performed according to the manufacturer's instructions and read using an ELISA microplate reader (Finstruments Multiskan Models 347; MTX Lab Systems, Inc., Vienna, VA, USA). Each experiment was performed in five wells and repeated at least three times.

Cell Migration Assay

The HUVEC migration study was performed using Transwells (Cat#3422; Corning, Tewksbury, MA, USA) as described previously.[23,24] Briefly, 5×10^4 cells in 200-μL serum-free medium were placed in the upper portion of a Transwell. The RPMI 1640 medium (containing 10% FBS) was placed in the bottom chamber at a final volume of 600 μL. All migration assays were conducted at 37°C for 6 hours, and the cells were then fixed in 4% paraformaldehyde (PFA) and stained with 4,6-diamidino-2-phenylindole (DAPI; Roche Diagnostics, Indianapolis, IN, USA). The cells that had not migrated through the membrane were removed with a cotton swab, and the membrane was imaged with fluorescence microscopy (Zeiss Axiophot, Thornwood, NY, USA). The HUVECs from five random fields of view were counted. Each experiment was repeated three times.

Tube Formation in HUVECs

Aliquots (150 μL) of Matrigel solution were poured into the 48-well plates (repeated two times), and the plates were incubated at 37°C for 1 hour in a 5% CO_2 incubator to form a Matrigel gel.[25] The HUVECs (1×10^4 per well) were seeded on the Matrigel, cultured in 1640 medium and incubated for 6 hours. The networks in Matrigel in five randomly chosen fields were counted and photographed under a microscope. In our study, the length of the capillary-like structures was measured from two-dimensional microscope images using ImageJ software. The experiments were repeated three times.

RNA Extraction and Relative Quantitative Real-Time PCR

Retinal and choroidal tissue and HUVECs were lysed in TRIzol (Invitrogen, Carlsbad, CA, USA), and RNA was extracted according to the manufacturer's protocol. Reverse transcriptase reactions were performed using a RevertAid First Strand cDNA Synthesis Kit with oligo-dT primer (Fermentas, Pittsburgh, PA, USA). Real-time PCR reactions were performed with SYBR Green PCR mix (Thermo, Pittsburgh, PA, USA) using an ABI7300 real-time PCR system (Applied Biosystems, Life Technologies, Foster City, CA, USA). The primers used in real-time PCR are shown in the Table. Data were normalized to the housekeeping genes human glyceraldehyde 3-phosphate dehydrogenase (GAPDH) and mouse β-actin, and relative multiples of changes in mRNA expression were determined by calculating fold change $= 2^{-\Delta\Delta ct}$. Each experiment was repeated five times.

Western Blot Analysis

Retinal and choroidal tissue and HUVECs were prepared with protein extraction and protease inhibitor kits (Pierce, Rockford, IL, USA). After centrifugation, the supernatant was collected, and the protein lysate was measured with a bicinchoninic acid (BCA) protein assay kit (Pierce) according to the manufacturer's instructions. Equal amounts of protein were separated by 12% SDS-PAGE and transferred electrophoretically to nitrocellulose membranes (Amersham, Little Chalfont, UK). The proteins were visualized with enhanced chemiluminescence Western blot (W-B) detection reagents (Pierce). Band densities were tested with antibodies against Slit2 (1:500, ab134166; Abcam, Cambridge, MA, USA), Robo1 (1:500, ab7279; Abcam), Robo4 (1:500, ab10547; Abcam), VEGF (1:200, ab46154; Abcam), VEGFR2 (1:1000, #55B11; Cell Signaling Technology [CST], Danvers, MA, USA), phosphoinositide 3 kinase (PI3K/AKT) (1:1000, #4685; CST), phosphorylated AKT (p-AKT) (1:1000, #4060; CST), p38 mitogen-activated protein kinases

Investigative Ophthalmology & Visual Science

TABLE. Gene Subtype Oligonucleotide Primers

Gene Subtype	Oligonucleotide Primers, 5′–3′	Size, bp
Human Slit2	F: CACCTCGTACAGCCGCACTT	107
	R: TGTGGACCGCTGAGGAGCAA	
Human Robo1	F: TCCTTGTGAGGGCAGCTAAT	145
	R: AGGTGCAGAACAGCATTTCC	
Human Robo4	F: CCCTGTGCTTGGAACTCAGTG	102
	R: CGCTGATGTACCCATAGGTGG	
Human VEGFA	F: GCTCTACTTCCCCAAATCACTG	105
	R: CTCTGACCCCGTCTCTCTCTT	
Human VEGFR2	F: GGAAGTGAGTGAAAGAGACACAG	103
	R: TGGGACATACACAACCAGAGAG	
Human AKT1	F: CACACCACCTGACCAAGATG	137
	R: CATCCCTCCAAGCTATCGTC	
Human MAPK1	F: GTTGCAGATCCAGACCATGA	107
	R: GACTTGGTGTAGCCCTTGGA	
Human GAPDH	F: GAGTCCACTGGCGTCTTCAC	120
	R: GTTCACACCCATGACGAACA	
Mouse Slit2	F: GACCAGAGTGGCTGACAAGAG	120
	R: GTGCCCTGATGGATGACTACTA	
Mouse Robo1	F: AGTTTCAAGGAGCAGACAGTGA	108
	R: CAGTCCCATTTCCATCATTCTT	
Mouse Robo4	F: CTCCTCGCTGTCATCCTTAGAG	101
	R: GTGTCTCCTCCCCATCACTG	
Mouse VEGFA	F: GACTGGATTCGCCATTTTCTTA	100
	R: GTGTATGTGGGTGGGTGTGTCT	
Mouse VEGFR2	F: TGGCAAATACAACCCTTCAGAT	100
	R: GTCACCAATACCCTTTCCTCAG	
Mouse AKT1	F: GTGGCAGGATGTGTATGAGAAG	145
	R: CTGGCTGAGTAGGAGAACTTGA	
Mouse MAPK1	F: CTTCCAACCTCCTGCTGAAC	103
	R: TCTGTCAAGAACCCTGTGTGAT	
Mouse β-actin	F: AGTGTGACGTTGACATCCGTA	112
	R: GCCAGAGCAGTAATCTCCTTCT	

F, forward; R, reverse.

(p38 MAPK) (1:1000, #8690; CST), phosphorylated p38 MAPK (p-p38 MAPK) (1:1000, #4511; CST), ERK1/2 (1:1000, #9102; CST), and phosphorylated ERK1/2 (p-ERK1/2) (1:1000, #4370; CST), followed by incubation with a horseradish peroxidase (HRP)-conjugated goat antibody against rabbit IgG (1:1000, #7074; CST). For sequential blotting with additional antibodies, the membranes were stripped with a restorative Western blot stripping buffer and reprobed with the indicated antibodies. Western blot analyses were repeated three times, and qualitatively similar results were obtained.

Statistical Analysis

Data analysis was performed using the statistical software Prism 5 (GraphPad Software, Inc., San Diego, CA, USA). All data are presented as the means ± SEM. Differences between experimental and control groups were made using the Mann-Whitney *U* test. A *P* value of less than 0.05 was considered to be statistically significant.

RESULTS

Slit2 Overexpression in Tg Mice and W-B Analysis of Pathway Molecules in Untreated Tg Mice and WT Mice

Western blot analysis was performed to assess the respective protein levels of Slit2, Robo receptors, VEGF, and VEGFR2, and the expression and phosphorylation of the signal transduction molecules AKT, p38MAPK, and ERK1/2 in untreated Tg and WT mice, with β-actin serving as an internal loading control. Six Tg mice (six eyes) and six WT mice were involved in this experiment. Our results showed that Slit2 protein expression was significantly increased in retinal and choroidal tissue of untreated Slit2 Tg mice compared with WT controls (increase to 2.69 ± 0.53, Slit2 group versus control, $P = 0.029$) (Figs. 1A, 1C). There was no significant difference in Robo1 ($P = 0.882$), Robo4 ($P = 0.343$), VEGF ($P = 0.384$), or VEGFR2 ($P = 0.343$) expression between the two untreated groups (Figs. 1A, 1C). Proteins downstream of VEGFR2, such as AKT, p38 MAPK, ERK1/2 and phosphorylation, were detected, and these pathway molecules remained at almost the same levels in the two untreated groups ($P > 0.05$) (Figs. 1B, 1D).

Laser-Treated Slit2 Tg Mice Developed More CNV Leakage Than the WT Mice

A laser-induced CNV model was developed in both Slit2 Tg and WT mice. Five lesions were made on one eye of each mouse. The area of CNV leakage was assessed by FA. Ten Tg mice (10 eyes) and 10 WT mice (10 eyes) were involved in FA analysis. Results showed that Slit2 Tg mice developed more fluorescein leakage from laser-induced CNV lesions than the WT mice (increase to 3.40 ± 1.34, Slit2 group versus control, $P < 0.0001$) (Fig. 2).

Robo1 and VEGFR2-ERK1/2 Signaling Pathways Were Upregulated in Retinal and Choroidal Tissue of Laser-Treated Slit2 Tg Mice

We investigated the possible mechanism underlying the observation that laser-treated Slit2 Tg mice developed more CNV than control mice. Quantitative real-time PCR (QRT-PCR) and Western blot analysis were performed to assess the respective mRNA and protein levels of the Robo receptors, VEGF, and VEGFR2, and the expression and phosphorylation of the signal transduction molecules AKT, p38 MAPK, and ERK1/2, with GAPDH or β-actin serving as an internal loading control. Ten laser-treated Tg mice (10 eyes) and 10 laser-treated WT mice (10 eyes) were involved in QRT-PCR analysis. Six laser-treated mice (six eyes) in each group were involved in the experiment of W-B. We found that Slit2 expression was upregulated in the retinal and choroidal tissue of laser-treated Slit2 Tg mice (W-B $P = 0.027$) and that Slit2 overexpression in CNV mice induced the upregulation of Robo1 (PCR $P = 0.010$, W-B $P = 0.027$) but not Robo4 (PCR $P = 0.131$, W-B $P = 0.882$) (Figs. 3A, 3B, 3D). Expression of VEGFR2 was significantly increased in the laser-treated Slit2 Tg group (PCR $P = 0.010$, W-B $P = 0.027$); however, there was no significant difference in VEGF expression between the two treated groups (PCR $P = 0.814$, W-B $P = 0.301$) (Figs. 3A, 3B, 3D). Proteins downstream of VEGFR2, such as AKT, p38 MAPK, and ERK1/2, were detected, and only ERK1/2 phosphorylation was increased (W-B $P = 0.027$), whereas AKT and p38 MAPK expression and phosphorylation remained at almost the same levels in the two treated groups ($P > 0.05$) (Figs. 3A, 3C, 3E).

Slit2 Overexpression Promoted Proliferation, Migration, and Tube Formation in HUVECs

We performed experiments to evaluate whether endogenous Slit2 overexpression had any effect on aspects of the angiogenic activities of HUVECs, such as proliferation, migration, and tube formation, in vitro. A CCK-8 Proliferation Assay Kit (Dojindo) was used to evaluate the effects of

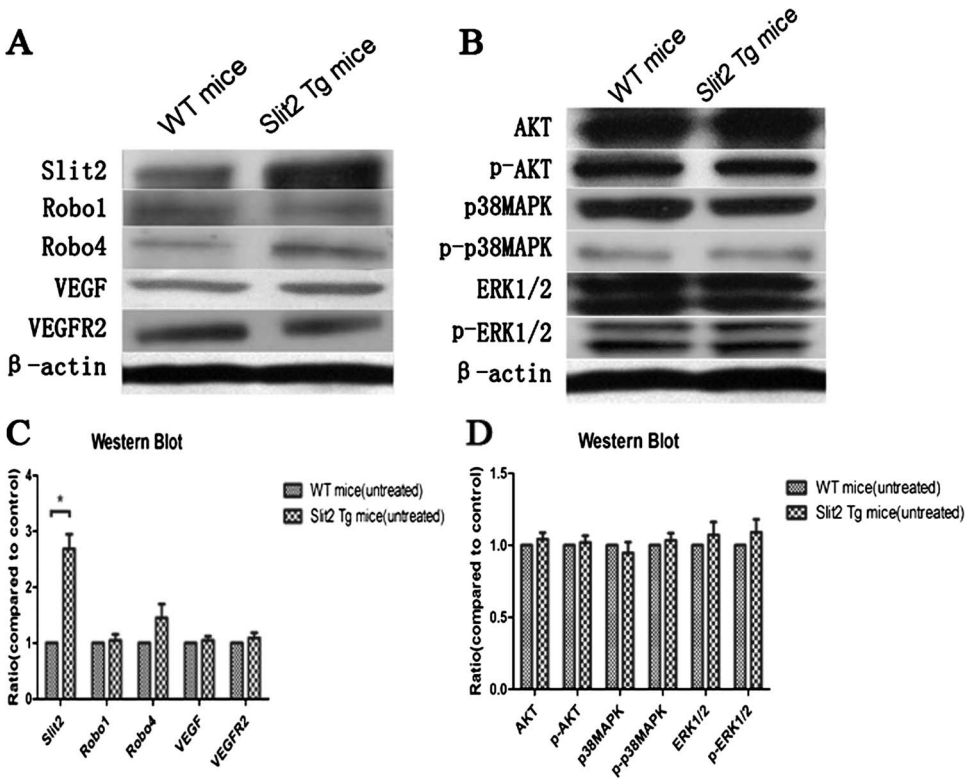

Figure 1. Untreated Slit2 Tg mice showed increased expression of Slit2 protein compared with the WT mice. (**A**, **B**) Representative blot images. (**C**, **D**) Results of statistical analysis of W-B data. Slit2 protein expression in retinal and choroidal tissue of untreated Slit2 Tg mice increase to 2.69 ± 0.53 compared with WT controls ($P = 0.029$) (**A**, **C**). There was no significant difference in Robo1 ($P = 0.882$), Robo4 ($P = 0.343$), VEGF ($P = 0.384$), or VEGFR2 ($P = 0.343$) expression between the two untreated groups (**A**, **C**). Proteins downstream of VEGFR2, such as AKT, p38 MAPK, ERK1/2, and phosphorylation were detected, and these pathway molecules remained at almost the same levels in the two untreated groups ($P > 0.05$) (**B**, **D**). Data are represented as the means ± SEM of fold changes compared with the controls. Each experiment was repeated at least three times. Six untreated mice (six eyes) were involved in each group. *$P < 0.05$.

endogenous Slit2 on HUVECs, and the results revealed that HUVECs transfected with the Slit2 plasmid increased proliferation compared with the control group (increase to 1.17 ± 0.06, Slit2 group versus control, $P = 0.004$) (Fig. 4A). The Boyden Chamber assay was used to evaluate effect of Slit2 on HUVEC migration. As shown in Figures 4B, 4D, and 4E, the number of Slit2-transfected cells that passed through the membrane was significantly higher than the number of control cells (increase to 1.59 ± 0.21, Slit2 group versus control, $P = 0.008$). A Matrigel assay was performed to evaluate the effect of endogenous Slit2 expression on tube formation in HUVECs. Slit2-transfected HUVECs showed an increased capacity to form a network compared with the negative control (increase to 1.84 ± 0.43, Slit2 group versus control, $P = 0.029$) (Figs. 4C, 4F, 4G). These results indicated that endogenous overexpression of Slit2 effectively promoted angiogenic activity in HUVECs.

Slit2 Overexpression in HUVECs Upregulated Both Robo1 and VEGFR2-ERK1/2 Signaling Pathway Expression in Slit2-Transfected HUVECs

As mentioned, Slit2 overexpression promoted CNV formation and vascular leakage in vitro through upregulation of Robo1 and VEGFR2, which activate phosphorylation of the downstream transduction molecule ERK1/2. To verify these results in vivo and to investigate a possible mechanism of endogenous Slit2 on the angiogenic activity of HUVECs, we performed QRT-PCR and W-B analyses to assess the respective mRNA (Fig. 5A) and protein (Figs. 5B–E) levels of the Robo receptors, VEGF, VEGFR2, and the expression and phosphorylation levels of AKT, p38 MAPK, and ERK1/2. We observed significant upregulation of Robo1 in Slit2-transfected HUVECs compared with untransfected HUVECs (PCR $P = 0.010$, W-B $P = 0.027$), whereas Robo4 expression remained almost the same in the two groups (PCR $P = 0.131$, W-B $P = 0.301$) (Figs. 5B, 5D). Consistent with our results in CNV mice, increased VEGFR2 (PCR $P = 0.010$, W-B $P = 0.027$) and pERK1/2 (W-B $P = 0.027$) expression levels were detected in Slit2-transfected HUVECs compared with the control group (Figs. 5B–E). Endogenous Slit2 overexpression did not impact VEGF, AKT, p38 MAPK, and ERK1/2 mRNA and protein expression in HUVECs, nor did it impact AKT and p38 MAPK phosphorylation ($P > 0.05$) (Figs. 5A–E).

Discussion

Recent studies have provided novel insights into the function of Slit2-Robo signaling in angiogenesis. However, Slit2 is reported to possess both pro- and antiangiogenic activities, and its role remains controversial. Slit2 protein has both attractive and repellent effects on endothelial cells.[13,17] In vivo studies have demonstrated that intraocular injection of the recombinant Slit2 protein decreased the risk of neovascular events[17]; however, a previous study also showed that Slit2 overexpression increased the lesion size of induced endometriosis in Tg mice.[22] Study of the function of Slit2 in the CNS has provided evidence that Slit2 stimulates motor axon fasciculation during muscle innervation, not by a classical

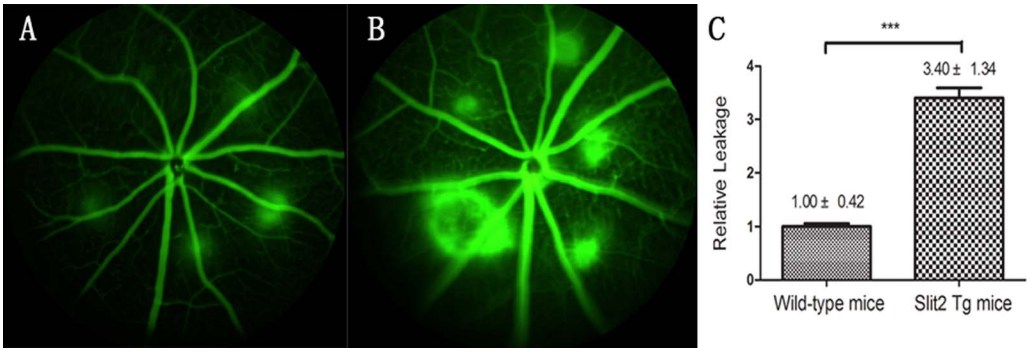

Figure 2. Laser-treated Slit2 Tg mice developed more CNV leakage than the wild-type controls. Fluorescein angiography analysis of CNV leakage was performed 14 days after laser photocoagulation in the Tg mice group and the control group. *Left*: Representative images of the retina fundus fluorescein angiography in different groups ([**A**] laser-treated WT mice; [**B**] laser-treated Slit2 Tg mice). (**C**) Results of statistical analysis. As shown in this figure, laser-treated Slit2 Tg mice developed more CNV leakage than the WT mice (***$P < 0.0001$). Ten laser-treated mice (10 eyes) were involved in each group. The data are presented as the means ± SD.

surround repulsion mechanism but by an autocrine mechanism, in which Slit2 produced by motor axons promotes their own fasciculation.[26] The contrary results obtained in previous studies indicated that endogenous Slit2 overexpression and the provision of exogenous recombinant Slit2 protein might have different effects on vascular formation and that they might function through different mechanisms. To investigate the specific effect of endogenous Slit2 on angiogenesis and its possible molecular mechanism, we used a Tg mouse line that overexpresses human Slit2[21] to construct a CNV mouse model, and plasmid-based gene transfer technology to increase Slit2 expression in HUVECs. Our results revealed that the Slit2 Tg mice showed more fluorescein leakage following laser-induced CNV lesions than the WT mice. Furthermore, Slit2 overexpression promoted the angiogenic activities of HUVECs, including proliferation, migration, and tube formation. These results indicated that the endogenous upregulation of Slit2 had proangiogenic functions both in vivo and in vitro. In this study, we also demonstrated that Slit2 promoted angiogenesis through the VEGFR2-ERK1/2 pathway.

Robo family members are trans-membrane receptors that interact with Slit2. Robo1 and Robo4 are expressed on the endothelial cell membrane and are thought to participate in physiological and pathological processes of vascular formation.[27–30] Previous studies have suggested that different regulatory effects of Slit2 on angiogenesis may be related to the various Robo receptors interacting with Slit2. It has been demonstrated that recombinant Slit2 protein promoted the migration and tube formation of endothelial cells in a Robo1-dependent manner,[13] but inhibited these processes in a Robo4-

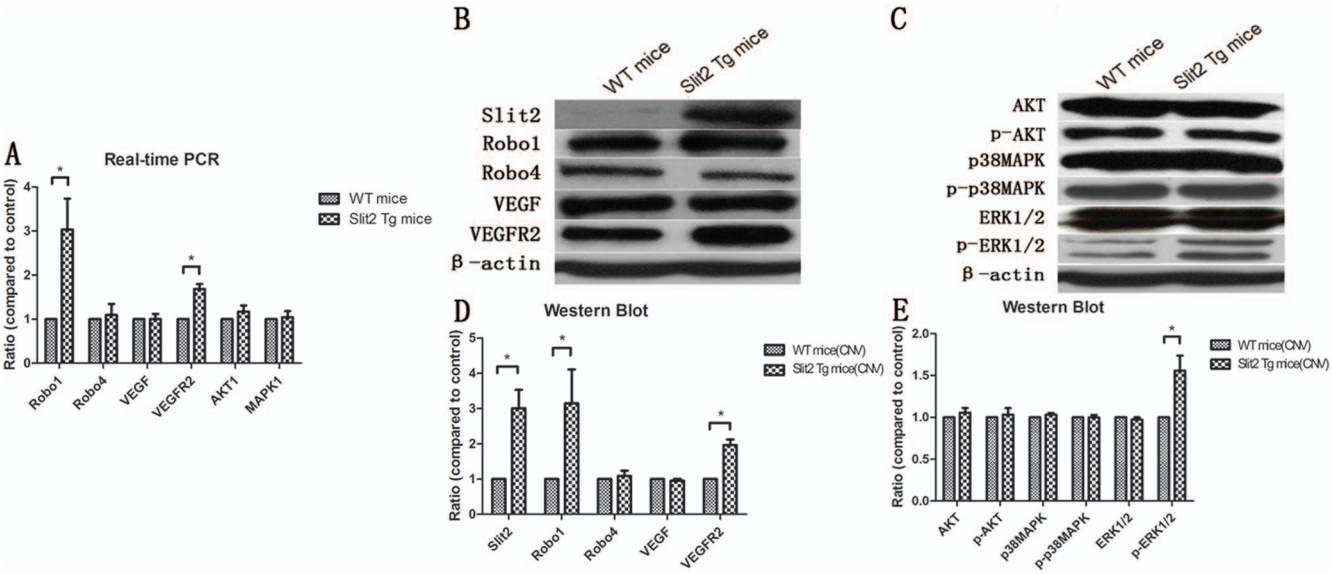

Figure 3. Robo1 and VEGFR2-ERK1/2 signaling pathways were upregulated in retinal and choroidal tissues of laser-treated Slit2 Tg mice. (**A**) Results of statistical analysis of QRT-PCR data. Slit2, Robo1, and VEGFR2 expression levels were upregulated in the laser-treated Slit2 group ($P = 0.010$), whereas Robo4 ($P = 0.131$), VEGF ($P = 0.814$), AKT1 ($P = 0.131$), and MAPK1 ($P = 0.666$) expression levels did not differ significantly between the two CNV groups. (**B**, **C**) Representative blot images and (**D**, **E**) results of statistical analysis of Western blot data. Robo1, VEGFR2, and p-ERK1/2 expression levels were upregulated in the laser-treated Slit2 group ($P = 0.027$), whereas Robo4 ($P = 0.882$), VEGF ($P = 0.301$), AKT ($P = 0.301$), p-AKT ($P = 0.301$), p38 MAPK ($P = 0.301$), p-p38 MAPK ($P = 0.882$), and ERK1/2 ($P = 0.301$) expression levels did not differ significantly between the two groups. Data are represented as the means ± SEM of fold changes compared with the controls. Each experiment was repeated at least three times. Ten laser-treated mice (10 eyes) were involved in each group in QRT-PCR analysis. The experiment of Western blot used six laser-treated mice (six eyes) in each group. *$P < 0.05$.

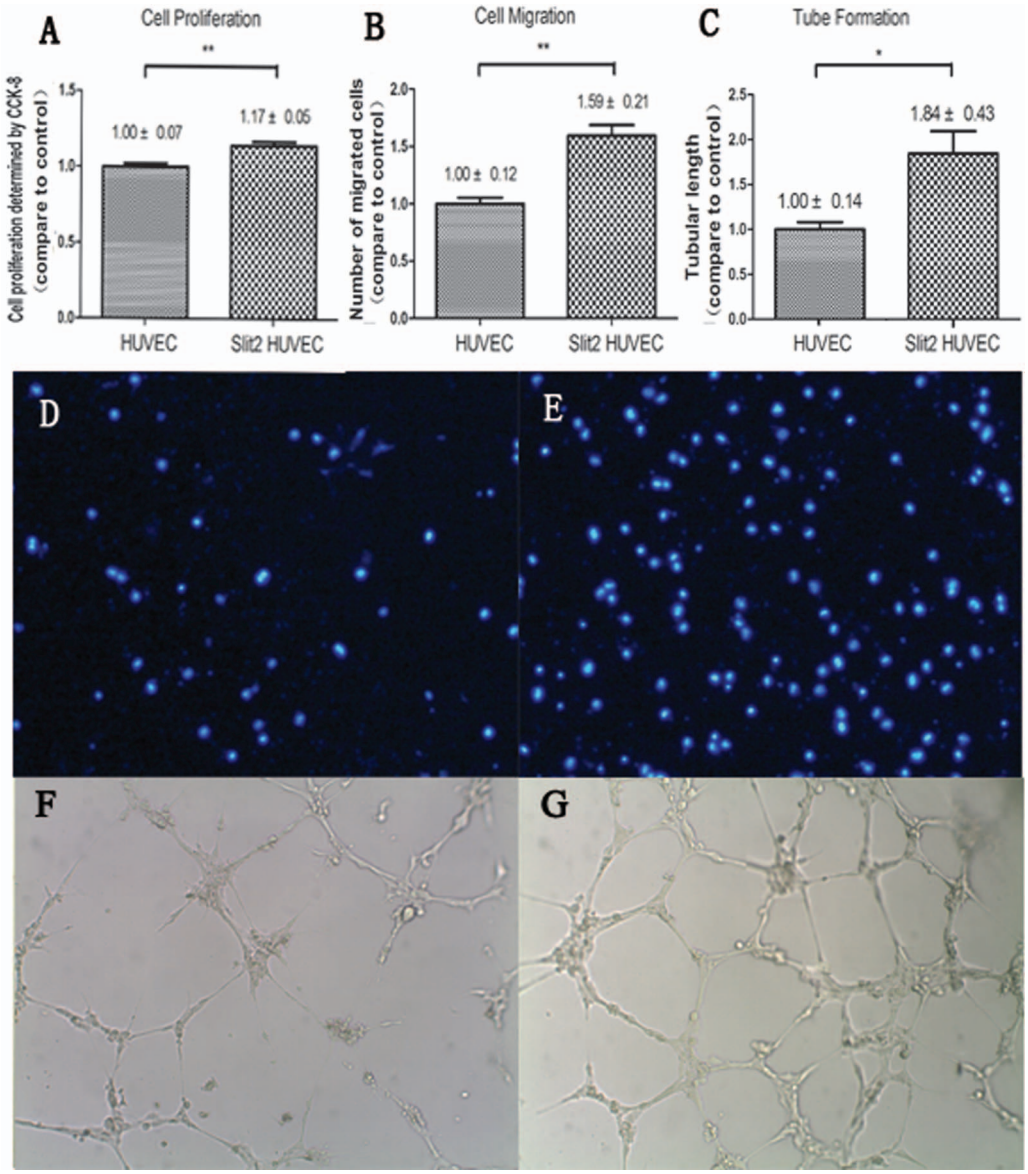

Figure 4. Slit2 overexpression promoted proliferation, migration, and tube formation in HUVECs. The results of the CCK-8 proliferation assay revealed that Slit2-transfected HUVECs displayed increased proliferation compared with the control group ($P = 0.004$) (**A**). Statistical analysis of the Boyden Chamber assay revealed that the number of cells that passed through the membrane in the Slit2-transfected group was significantly higher than the number in the control group ($P = 0.008$) ([**B**] statistical analysis; [**D**] HUVEC; [**E**] Slit2-HUVEC). In the Matrigel assay, Slit2-transfected HUVECs exhibited an increased capacity to form a network compared with the negative control ($P = 0.029$) ([**C**] statistical analysis; [**F**] HUVEC; [**G**] Slit2-HUVEC). The data are presented as the means ± SEM. Each experiment was repeated at least three times. $^{*}P < 0.05$, $^{**}P < 0.01$.

dependent manner.[17] However, in the present study, endogenous Slit2 upregulation in HUVECs increased Robo1 but not Robo4 expression, and similar Robo1 overexpression was detected in the CNVs of Slit2 Tg mice. These results suggested that Robo1, but not Robo4, contributes to the angiogenesis and vascular leakage induced by endogenous Slit2.

The VEGFA, which has three receptors (VEGFR1–3), is a strong regulator of vascular formation. Previous studies have demonstrated that the in vivo angiogenic response to VEGFA is mainly mediated by VEGFR2.[31] This response relies on the activation of VEGFR2 and involves many downstream effectors, including PI3K/AKT, p38 MAPK, and ERKs.[32–34] Previous studies also have shown that the function of Slit2-Robo signaling in angiogenesis may be dependent on its interfering with the VEGF pathway. An in vitro study showed that the activation of Slit2-Robo4 signaling in endothelial cells failed to activate the MAPK pathway after VEGF treatment,[35] and that the proangiogenic function of recombinant Slit2 on HUVECs could be blocked by PI3K/AKT inhibitor.[36] However, the specific mechanism underlying Slit2 interference with the VEGF pathway is still unclear. We used a laser-induced CNV mouse model in which VEGF was the major stimulator of angiogenesis,[37] and found that Slit2 Tg mice developed more CNV than WT mice. Laser-treated Slit2 Tg mice also had increased VEGFR2 but not VEGFA expression, whereas endogenous Slit2 overexpression promoted the biological activity of HUVECs and upregulated VEGFR2 expression. Our results also demonstrated that Slit2 upregulation increased ERK1/2 but not AKT or p38 MAPK phosphorylation both in vivo and in vitro. These results were different from the results

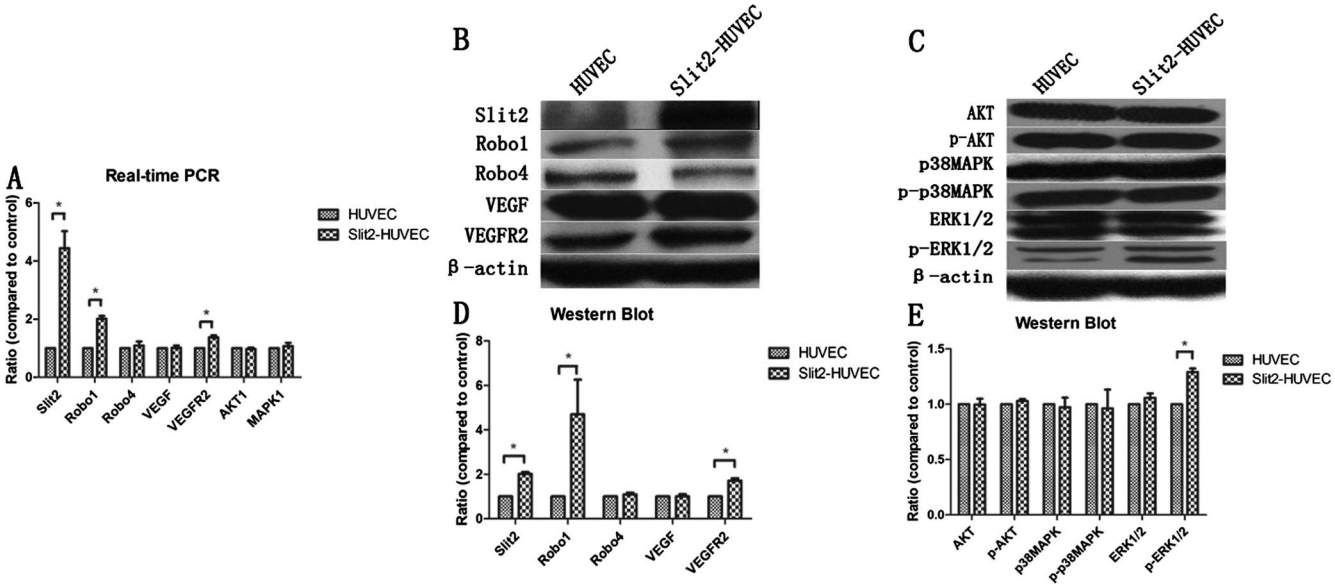

Figure 5. Slit2 overexpression in HUVECs upregulated both Robo1 and VEGFR2-ERK1/2 signaling pathway expression in Slit2-transfected HUVECs. (**A**) Results of statistical analysis of QRT-PCR data. As shown in this figure, Slit2, Robo1, and VEGFR2 expression levels were upregulated in the Slit2 group ($P = 0.010$), whereas Robo4, VEGF, AKT1, and MAPK1 expression levels did not differ significantly between the two groups ($P = 0.131$). (**B**, **C**) Representative blot images, and (**D**, **E**) results of statistical analysis of Western blot data. As shown in this figure, Slit2, Robo1, VEGFR2, and p-ERK1/2 expression levels were upregulated in the Slit2 group ($P = 0.027$), whereas Robo4 ($P = 0.301$), VEGF ($P = 0.301$), AKT ($P = 0.882$), p-AKT ($P = 0.301$), p38 MAPK ($P = 0.301$), p-p38 MAPK ($P = 0.882$), and ERK1/2 ($P = 0.301$) expression levels did not differ significantly between the two groups. Data are represented as the means ± SEM of fold changes compared with the controls. Each experiment was repeated at least three times. $^*P < 0.05$.

reported in previous studies. We speculate that, in different contexts, such as different diseases or the manner of Slit2 expression (i.e., endogenous or exogenous), Robo receptors respond to Slit2 differently. In addition, downstream effectors of VEGFR2, such as AKT, p38 MAPK, and ERK1/2, might play complex roles in regulating angiogenesis and vascular permeability and might be further selectively activated by Robo receptors in different circumstances. Our findings revealed that endogenous Slit2 overexpression upregulated Robo1 receptor expression and might have a proangiogenic function via activation of the VEGFR2-ERK1/2 signaling pathway. However, HUVECs used in the in vitro study were macrovascular cells and had limitation for studies of retinal neovascularization and CNV.

In conclusion, we identified the involvement of Slit2-Robo1 signaling in angiogenesis and suggested that endogenous Slit2 overexpression promoted angiogenesis and vascular leak through selective upregulation of Robo1 and VEGFR2 expression, which led to activation of the ERK1/2 pathway. Slit2 performed complicated functions in angiogenesis, and further studies are required to investigate the detailed mechanism of Slit2 protein and its Robo receptors, which may be important for better understanding the role of this signaling pathway in vascular disease and for the development of clinical therapeutic tools.

Acknowledgments

We thank Lijing Wang and Xiaodong He, Vascular Biology Research Institute, Guangdong Pharmaceutical University, for their help in transportation of the Tg mice.

Supported by the National Basic Research Program of China (973 Program, 2011CB510200) and the National Natural Science Foundation of China (Grant 81100666). The organizations that funded this study had no role in the study design, data collection, and analysis or in the decision to publish or prepare the manuscript.

Disclosure: **S. Li**, None; **L. Huang**, None; **Y. Sun**, None; **Y. Bai**, None; **F. Yang**, None; **W. Yu**, None; **F. Li**, None; **Q. Zhang**, None; **B. Wang**, None; **J.-G. Geng**, None; **X. Li**, None

References

1. Klettner A, Kauppinen A, Blasiak J, Roider J, Salminen A, Kaarniranta K. Cellular and molecular mechanisms of age-related macular degeneration: from impaired autophagy to neovascularization. *Int J Biochem Cell Biol*. 2013;45:1457–1467.
2. Witmer AN, Vrensen GF, Van Noorden CJ, Schlingemann RO. Vascular endothelial growth factors and angiogenesis in eye disease. *Prog Retin Eye Res*. 2003;22:1–29.
3. Penn JS, Madan A, Caldwell RB, Bartoli M, Caldwell RW, Hartnett ME. Vascular endothelial growth factor in eye disease. *Prog Retin Eye Res*. 2008;27:331–371.
4. Schwesinger C, Yee C, Rohan RM, et al. Intrachoroidal neovascularization in transgenic mice overexpressing vascular endothelial growth factor in the retinal pigment epithelium. *Am J Pathol*. 2001;158:1161–1172.
5. Brose K, Bland KS, Wang KH, et al. Slit proteins bind Robo receptors and have an evolutionarily conserved role in repulsive axon guidance. *Cell*. 1999;96:795–806.
6. Kidd T, Bland KS, Goodman CS. Slit is the midline repellent for the robo receptor in *Drosophila*. *Cell*. 1999;96:785–794.
7. Kidd T, Brose K, Mitchell KJ, et al. Roundabout controls axon crossing of the CNS midline and defines a novel subfamily of evolutionarily conserved guidance receptors. *Cell*. 1998;92:205–215.
8. Wu W, Wong K, Chen J, et al. Directional guidance of neuronal migration in the olfactory system by the protein Slit. *Nature*. 1999;400:331–336.
9. Hohenester E. Structural insight into Slit-Robo signalling. *Biochem Soc Trans*. 2008;36:251–256.

10. Wong K, Ren XR, Huang YZ, et al. Signal transduction in neuronal migration: roles of GTPase activating proteins and the small GTPase Cdc42 in the Slit-Robo pathway. *Cell*. 2001; 107:209–221.
11. Tole S, Mukovozov IM, Huang YW, et al. The axonal repellent, Slit2, inhibits directional migration of circulating neutrophils. *J Leukoc Biol*. 2009;86:1403–1415.
12. Huminiecki L, Gorn M, Suchting S, Poulsom R, Bicknell R. Magic roundabout is a new member of the roundabout receptor family that is endothelial specific and expressed at sites of active angiogenesis. *Genomics*. 2002;79:547–552.
13. Wang B, Xiao Y, Ding BB, et al. Induction of tumor angiogenesis by Slit-Robo signaling and inhibition of cancer growth by blocking Robo activity. *Cancer Cell*. 2003;4:19–29.
14. Yuen DA, Robinson LA. Slit2-Robo signaling: a novel regulator of vascular injury. *Curr Opin Nephrol Hypertens*. 2013;22: 445–451.
15. Jones CA, Nishiya N, London NR, et al. Slit2-Robo4 signalling promotes vascular stability by blocking Arf6 activity. *Nat Cell Biol*. 2009;11:1325–1331.
16. Sheldon H, Andre M, Legg JA, et al. Active involvement of Robo1 and Robo4 in filopodia formation and endothelial cell motility mediated via WASP and other actin nucleation-promoting factors. *FASEB J*. 2009;23:513–522.
17. Jones CA, London NR, Chen H, et al. Robo4 stabilizes the vascular network by inhibiting pathologic angiogenesis and endothelial hyperpermeability. *Nat Med*. 2008;14:448–453.
18. Suchting S, Heal P, Tahtis K, Stewart LM, Bicknell R. Soluble Robo4 receptor inhibits in vivo angiogenesis and endothelial cell migration. *FASEB J*. 2005;19:121–123.
19. Koch AW, Mathivet T, Larrivee B, et al. Robo4 maintains vessel integrity and inhibits angiogenesis by interacting with UNC5B. *Dev Cell*. 2011;20:33–46.
20. Plump AS, Erskine L, Sabatier C, et al. Slit1 and Slit2 cooperate to prevent premature midline crossing of retinal axons in the mouse visual system. *Neuron*. 2002;33:219–232.
21. Han HX, Geng JG. Over-expression of Slit2 induces vessel formation and changes blood vessel permeability in mouse brain. *Acta Pharmacol Sin*. 2011;32:1327–1336.
22. Guo SW, Zheng Y, Lu Y, Liu X, Geng JG. Slit2 overexpression results in increased microvessel density and lesion size in mice with induced endometriosis. *Reprod Sci*. 2013;20:285–298.
23. Bai Y, Yu W, Han N, et al. Effects of semaphorin 3A on retinal pigment epithelial cell activity. *Invest Ophthalmol Vis Sci*. 2013;54:6628–6638.
24. Bai YJ, Huang LZ, Xu XL, et al. Polyethylene glycol-modified pigment epithelial-derived factor: new prospects for treatment of retinal neovascularization. *J Pharmacol Exp Ther*. 2012; 342:131–139.
25. Cheng Y, Huang L, Li X, Zhou P, Zeng W, Zhang C. Genetic and functional dissection of ARMS2 in age-related macular degeneration and polypoidal choroidal vasculopathy. *PLoS One*. 2013;8:e53665.
26. Jaworski A, Tessier-Lavigne M. Autocrine/juxtaparacrine regulation of axon fasciculation by Slit-Robo signaling. *Nat Neurosci*. 2012;15:367–369.
27. Kidd T, Brose K, Mitchell KJ, et al. Roundabout controls axon crossing of the CNS midline and defines a novel subfamily of evolutionarily conserved guidance receptors. *Cell*. 1998;92: 205–215.
28. Brose K, Bland KS, Wang KH, et al. Slit proteins bind Robo receptors and have an evolutionarily conserved role in repulsive axon guidance. *Cell*. 1999;96:795–806.
29. Li HS, Chen JH, Wu W, et al. Vertebrate slit, a secreted ligand for the transmembrane protein roundabout, is a repellent for olfactory bulb axons. *Cell*. 1999;96:807–818.
30. Plump AS, Erskine L, Sabatier C, et al. Slit1 and Slit2 cooperate to prevent premature midline crossing of retinal axons in the mouse visual system. *Neuron*. 2002;33:219–232.
31. Claesson-Welsh L, Welsh M. VEGFA and tumour angiogenesis. *J Intern Med*. 2013;273:114–127.
32. Jiang BH, Liu LZ. PI3K/PTEN signaling in angiogenesis and tumorigenesis. *Adv Cancer Res*. 2009;102:19–65.
33. Ballmer-Hofer K, Andersson AE, Ratcliffe LE, Berger P. Neuropilin-1 promotes VEGFR-2 trafficking through Rab11 vesicles thereby specifying signal output. *Blood*. 2011;118:816–826.
34. Takahashi T, Yamaguchi S, Chida K, Shibuya M. A single autophosphorylation site on KDR/Flk-1 is essential for VEGF-A-dependent activation of PLC-gamma and DNA synthesis in vascular endothelial cells. *EMBO J*. 2001;20:2768–2778.
35. Fish JE, Wythe JD, Xiao T, et al. A Slit/miR-218/Robo regulatory loop is required during heart tube formation in zebrafish. *Development*. 2011;138:1409–1419.
36. Li Y, Fu S, Chen H, et al. Inhibition of endothelial Slit2/Robo1 signaling by thalidomide restrains angiogenesis by blocking the PI3K/Akt pathway. *Dig Dis Sci*. 2014;59:2958–2966.
37. Kwak N, Okamoto N, Wood JM, Campochiaro PA. VEGF is major stimulator in model of choroidal neovascularization. *Invest Ophthalmol Vis Sci*. 2000;41:3158–3164.

Investigative Ophthalmology & Visual Science